Study on the Indoor Thermal Environment of Prefabricated Railway Buildings in High-Altitude Cold Regions

Hui Li , Lintao Ma , Haojie Zhang , Zhixiang Yu , Hu Xu *

Posted Date: 23 March 2026

doi: 10.20944/preprints202603.1682.v1

Keywords: railway building; prefabricated structure; indoor thermal environment; thermal bridge; extreme environments

 doi:10.20944/preprints202603.1682.v1

Article

Study on the Indoor Thermal Environment of Prefabricated Railway Buildings in High-Altitude Cold Regions

Hui Li [1,2], Lintao Ma [1], Haojie Zhang [1], Zhixiang Yu [1] and Hu Xu [1,*]

[a] School of Civil Engineering, Southwest Jiaotong University, Chengdu 610031, P. R. China

[b] China Railway First Survey & Design Institute Group Co., Xi'an 710043, P. R. China

* Correspondence: xuhu@swjtu.edu.cn

Abstract

Prefabricated buildings offer high industrialization and construction efficiency, making them well-suited for adverse construction conditions. As railway networks expand into western China's high-altitude regions, prefabricated structures have been increasingly adopted for living quarters along railway lines in cold, high-altitude areas. This study investigated the energy consumption characteristics of such buildings by simulating the thermal performance of prefabricated exterior walls, using the average heat-transfer coefficient with particular attention to thermal-bridge effects at wall junctions. Indoor thermal-environment analysis was conducted using DeST software, and the methodology was validated against field-measurement data. Furthermore, taking a railway living-quarters building as a case study, this study analyzed the key factors and their influence patterns on the indoor thermal environment under high-altitude cold conditions. Results show that local average temperature distributions vary significantly with room orientation; building orientation, south-facing window-to-wall ratio, and exterior-wall heat-transfer coefficient markedly affect overall average indoor temperature and energy consumption. Adjusting these design parameters can effectively improve indoor comfort and reduce energy use. Finally, through simulation of buildings in typical high-altitude cold locations (Litang, Batang, Qamdo, Nyingchi, and Lhasa), specific measures are proposed to enhance the indoor thermal environment of buildings in the western Sichuan plateau.

Keywords: railway building; prefabricated structure; indoor thermal environment; thermal bridge; extreme environments

1. Introduction

China's total railway mileage has grown substantially in recent years, exceeding 160,000 km. As railway development extends into western China, many sections traverse plateaus above 3,000 m, classified as cold or severe-cold zones, particularly in the Ganzi region. These areas present challenging construction conditions and limited availability of building materials. Prefabricated construction offers advantages such as rapid assembly and energy efficiency [1,2], making it suitable for deployment along railway lines in high-altitude cold regions. However, the harsh climate and complex natural environment in these areas pose significant challenges for indoor thermal-environment design and energy-consumption control [3].

Field surveys reveal a widespread discrepancy between indoor thermal conditions and resident comfort requirements. Studies of residents in the Kham region indicate that the main heating season lasts from mid-October to mid-March; over 38.1% of residents describe winter indoor temperatures as cold, resulting in a thermal-dissatisfaction rate of 42.9% [4]. Measurements in Danba County further demonstrate that without active heating, average indoor temperatures reach only approximately 5.93 °C, that is merely 1 °C higher than outdoors, with residents explicitly expressing

 doi:10.20944/preprints202603.1682.v1

needs for warmer conditions [5]. Winter comfort assessments confirm that without heating equipment, indoor temperatures fall far below the lower acceptable threshold (9.75 °C). Even with intermittent use of air-conditioners or electric heaters, indoor temperatures only occasionally reach acceptable comfort ranges. Comparisons of Thermal Sensation Vote (TSV) values from surveys in Kangding County and Ganzi County with Predicted Mean Vote (PMV) values indicate that, during winter under the low-pressure, low-oxygen conditions of the Sichuan-Tibet plateau, residents exhibit relatively low satisfaction with indoor thermal comfort. In summary, residents in high-altitude cold areas of Ganzi County are generally dissatisfied with their indoor thermal environments. This problem is particularly acute in prefabricated housing, where modular construction may exacerbate issues such as inadequate insulation, heat leakage through joints, and increased central-heating energy consumption [6,7].

Scholars worldwide have conducted extensive research on the indoor thermal environment of prefabricated structures. Zhu et al. [8] investigated exterior-wall and roof configurations for prefabricated composite-wall systems and, based on characteristics of different climate zones in China, proposed corresponding insulation materials and thicknesses for practical reference. Ju et al. [9] studied prefabricated concrete buildings in cold regions, exploring optimal insulation-layer thickness ranges in building envelopes to achieve significant overall energy savings. Yang et al. [10] analyzed thermal bridges in prefabricated building envelopes through temperature-field and heat-flux simulations, examining the impact of balconies, air-conditioning panels, and bay windows on thermal performance, and demonstrating the benefits of thermal breaks at bridge locations for reducing energy consumption. Hu et al. [11] investigated thermal bridge effects at vertical joints in dry-connected prefabricated structures and suggested external-insulation measures for T-joint wall panels. Scioti et al. [12] optimized the material composition of a high-performance prefabricated load-bearing wall to improve thermal performance while maintaining mechanical strength, adopting construction details to reduce the effect of thermal bridge at wall joints. Bouchlaghem et al. [13] used numerical simulation to optimize thermal performance of building envelopes, determining optimal parameters to enhance indoor comfort and satisfaction. Yu et al. [14] summarized life-cycle energy-saving and emission-reduction performance of common prefabricated concrete sandwich panels and light-steel-frame buildings in China, addressing thermal-environment and energy-consumption issues, and recommended further study of thermal environments in prefabricated buildings with different structures and functions. Overall, existing literature focuses primarily on analyzing impacts of local characteristics and specific construction details of prefabricated residential structures on indoor thermal environments; research on railway buildings remains scarce, particularly regarding their indoor thermal environment and energy consumption under high-altitude cold conditions.

This paper selects a typical reinforced concrete frame building along a railway line and establishes a numerical model that accounts for the thermal bridge effect of the prefabricated envelope, as shown in Figure 1. It investigates the overall thermal performance and energy consumption of the building in the high-altitude cold environment of the Ganzi region. By analysing the functional and energy-use characteristics of railway-adjacent buildings and incorporating energy-saving design principles for plateau areas, the study aims to identify key design factors and their influence patterns, providing a reference for the architectural design of railway prefabricated bulidings in western China's high-altitude cold regions.

 doi:10.20944/preprints202603.1682.v1

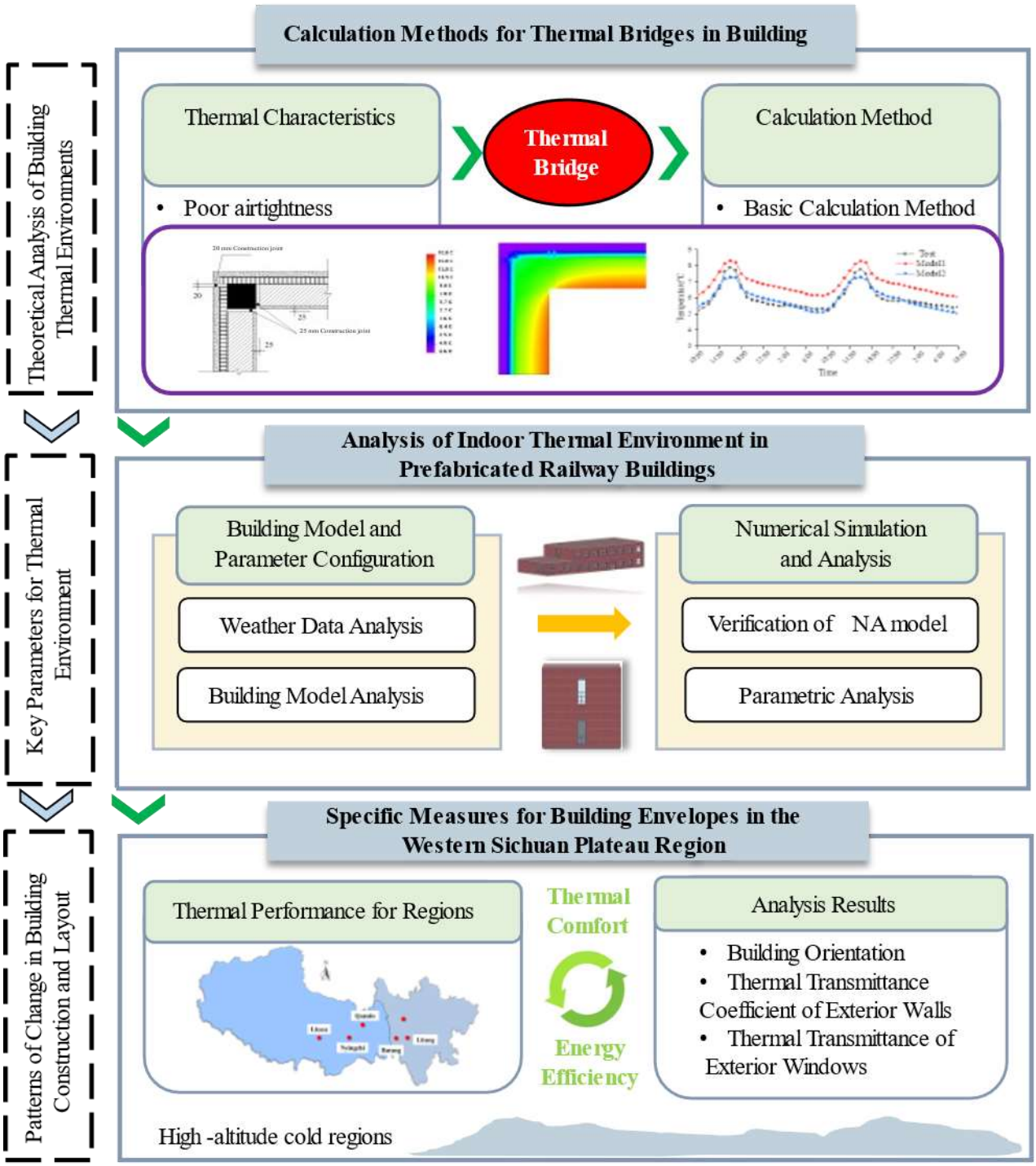

Figure 1. Technical roadmap.

3. Calculation Methods for Thermal Bridges in Buildings

Compared to traditional cast-in-place construction, prefabricated structures incorporate more joints, nodes, and connectors. Gaps at these connection points not only directly affect seismic, wind-resistant, and waterproof performance of prefabricated components [15], but also influence indoor thermal environment. Poor airtightness increases indoor-outdoor air exchange rates, particularly in cold regions, leading to rapid heat loss, significant temperature drops, and substantially increased heating energy consumption. Therefore, building airtightness should meet regulatory thresholds [16]. Certain components within building envelopes exhibit significantly different thermal conductivity compared to primary wall materials. Under substantial indoor-outdoor temperature differences, these areas experience concentrated heat flow, leading to larger temperature differentials

 doi:10.20944/preprints202603.1682.v1

between inner and outer surfaces, forming thermal bridges [17]. During winter, heat escapes rapidly through these bridges; in summer, external heat transfers inward, increasing heating or cooling energy demands.

In practice, various connection components and filler materials are often employed to meet airtightness requirements. However, the impact of thermal bridges is frequently overlooked in the thermal analysis of prefabricated structures. Structural thermal bridges are particularly prone to forming at corners, window-wall junctions, bay windows, and balconies within the building envelope, contributing to energy loss [18], as illustrated in Figure 2.

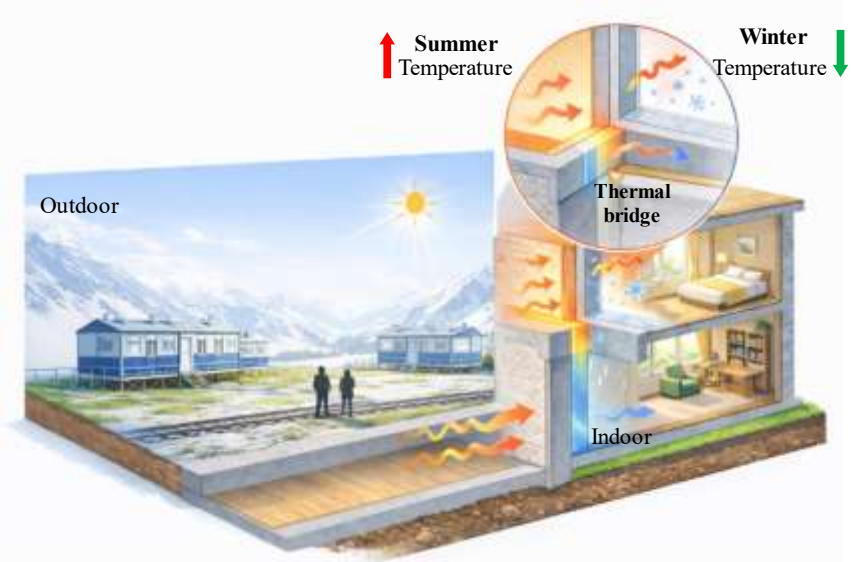

Figure 2. Basic Calculation Method.

The current standard GB50176-2016 Thermal Design Code for Civil Buildings [19] recommends using the average thermal transmittance coefficient (Km) of the envelope to account for thermal bridge effects. The calculation formula is given in Equation (1):

$$K_{\mathrm{m}} = K + \frac{\sum \psi_j l_j}{A} \tag{1}$$

where K is the thermal transmittance coefficient of the plain wall section, W/(m²·K); l_j is the length of structural thermal bridge; A is the area of the envelope element, m²; ψ_j is the linear thermal transmittance coefficient of the structural thermal bridge.

This method introduces the linear thermal transmittance coefficient (ψ) to quantify the influence of thermal bridges on the plain wall section. The standard [19] provides the calculation method for ψ at different junction details, as shown in Equation (2):

$$\psi = \frac{Q^{2D} - KA(t_i - t_e)}{l(t_i - t_e)} = \frac{Q^{2D}}{l(t_i - t_e)} - KC \tag{2}$$

where ψ is the linear thermal transmittance of the thermal bridge, W/(m²·K); Q^{2D} is the heat transfer rate through the thermal bridge of the building envelope, W; K is the thermal transmittance of the planar part of the building envelope, W/(m²·K); A is the area of the building envelope used for calculating Q^{2D}, m²; t_i is the indoor air temperature on the interior side of the building envelope, °C; t_e is the outdoor air temperature on the exterior side of the building envelope, °C; l is the length of the building envelope used for calculating Q^{2D}, m; C is the width of the building envelope used for calculating Q^{2D}, m.

Given the complexity of calculating ψ analytically, the software PTemp can be used for precise modeling and computation of specific thermal bridge details. Key boundary parameters are set as

 doi:10.20944/preprints202603.1682.v1

follows: (1) Interior surface with a convective heat transfer coefficient of 23.0 W/(m²·K). The indoor design temperature for winter is typically taken as 18 °C; (2) Exterior surface with a convective heat transfer coefficient of 8.7 W/(m²·K). Outdoor design temperature t_e is determined based on the average temperature of the coldest period, historically defined as the period with a non-exceedance probability of 5 days per year, calculated as:

$$t_e = 0.3t_w + 0.7t_{e\,min} \quad (3)$$

where t_w is the outdoor design temperature for heating, °C; $t_{e,min}$ is the cumulative minimum daily mean temperature, °C.

3.2. Validation of the Calculation Method

To validate the method, a prefabricated building [20] was selected to simulate using both DeST and PTemp software, and the results were compared against the field data.

3.2.1. Description of the Measured Building

The building, located in Weinan City, Shaanxi Province, is a residential structure in the Huizhou architectural style. Its main structure combines a cast-in-place reinforced concrete frame with prefabricated composite wall panels, which consist of concrete ribs and lightweight blocks. It has a flat roof, two stories (each 3.3 m high), and identical window-to-wall ratios on both floors: 0.06 (east), 0.06 (west), 0.26 (north), and 0.28 (south). All windows have a sill height of 0.9 m and a width of 2.1 m, with heights of either 1.5 m or 0.9 m. The three-dimensional diagram and first-floor plan is shown in Figure 3.

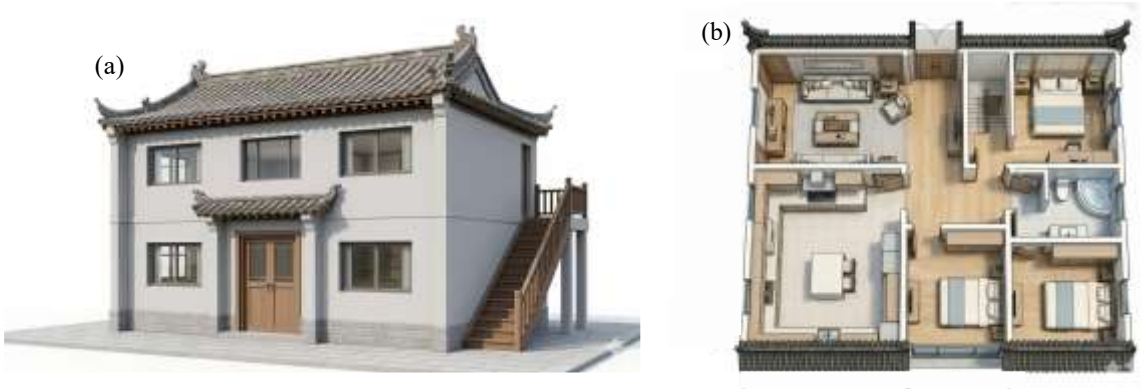

Figure 3. Architectural plan layout. (a) Three-dimensional diagram (b) Floor plan.

Continuous 48-hour on-site measurements were conducted, across seven rooms on both floors. Results indicated that the average temperature on the first floor was significantly higher than on the second, and south-facing rooms were warmer than others. For analysis, Bedroom B on the first floor was selected for comparison between simulation and measurement.

3.2.2. Calculation of the Average Thermal Transmittance K_m

The exterior wall uses a prefabricated sandwich insulation system, consisting of 180 mm composite panel as inner leaf, 50 mm EPS board, and 45 mm fine-aggregate reinforced concrete as outer leaf, finished internally with 20 mm rendering, yielding a wall *K* value equal to 0.579 W/(m²·K). Interior walls are 160 mm composite panels with 20 mm rendering on both sides, yielding a wall *K* value equal to 1.971 W/(m²·K). Exterior windows are double-glazed plastic-steel units with aluminum alloy frames, yielding a wall *K* value equal to 1.698 W/(m²·K).

Using the PTemp two-dimensional steady-state heat transfer software, the thermal bridge linear heat transfer coefficient ψ_j at the local connection points between exterior wall-exterior wall, exterior wall-interior wall, and exterior wall-exterior window was calculated, as shown in Figure 4. Taking

 doi:10.20944/preprints202603.1682.v1

the exterior wall external corner as an example, its planar construction is shown in Figure 4 (a). The model was created based on actual component dimensions, with construction joints filled using cement mortar as depicted in Figure 4 (b). The temperature distribution at the thermal bridge is illustrated in Figure 4 (c), yielding a calculated structural thermal bridge line heat transfer coefficient of 0.16 W/(m·K). Using the same method, the linear heat transfer coefficients for the thermal bridges at the exterior wall-interior wall and exterior wall-exterior window junctions were calculated as 0.14 W/(m·K) and 0.19 W/(m·K), respectively, as shown in Table 1. Based on these values, the average heat transfer coefficient K_m for the exterior envelope structure was calculated using Equation (1) to be 0.642 W/(m²·K).

Table 1. verage Thermal Transmittance Coefficient K_m.

Thermal Bridge Location	Ψ_j / W/(m·K)	$\Psi_j l_j$ / W/K	$\psi_j l_j$/A / W/(m²·K)
Exterior Wall - Exterior Wall	0.16	0.16	0.019
Exterior Wall - Interior Wall	0.14	0.14	0.017
Exterior Wall - Exterior Window	0.19	0.228	0.027
$\Sigma\psi_j l_j$/A			0.063

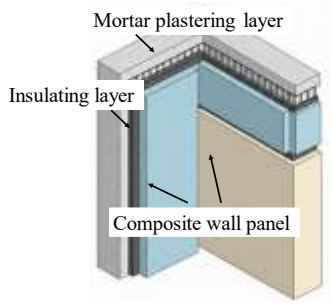

(a) Construction at exterior wall external corners

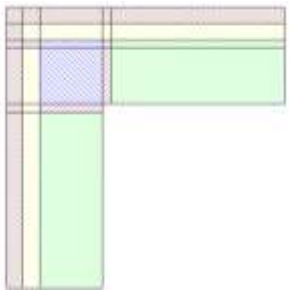

(b) Model at the exterior wall corner

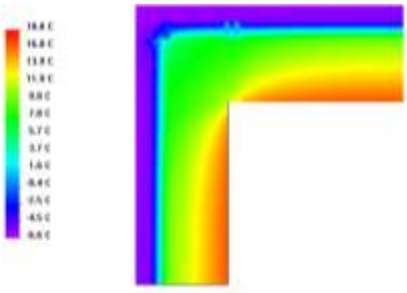

(c) Thermal bridge temperature distribution

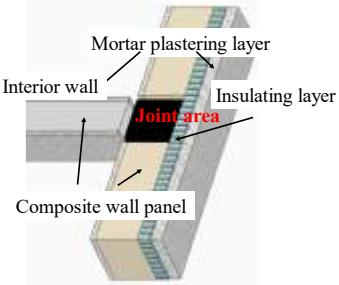

(d) Exterior Wall-Interior Wall Joint Construction

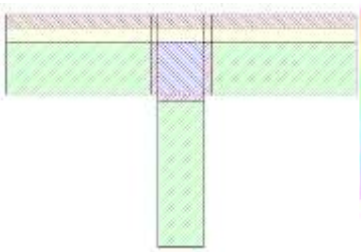

(e) Exterior Wall-Interior Wall Joint Thermal Bridge Model

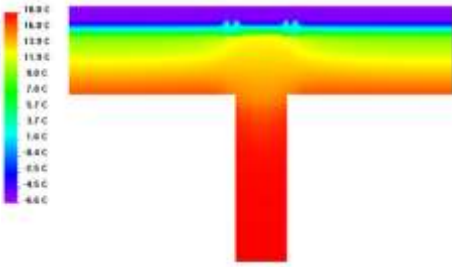

(f) Thermal Bridge Temperature Distribution

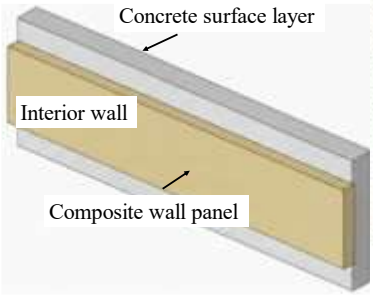

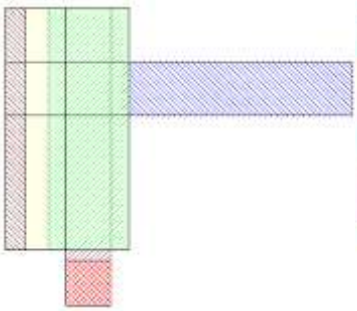

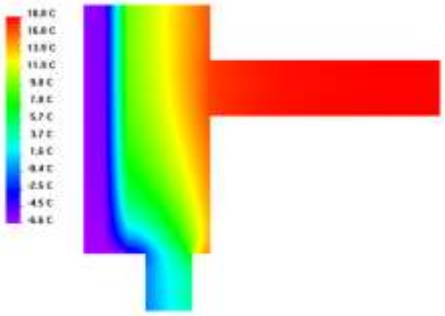

 doi:10.20944/preprints202603.1682.v1

(g) External Structure | (h) Thermal Bridge Model at Exterior Wall-Exterior Window Joint | (i) Thermal Bridge Temperature Distribution

Figure 4. Analysis on the thermal bridge.

3.2.3. DeST Modeling and Parameter Settings

DeST is a commonly used software for building thermal environment analysis. Its core technology employs a three-dimensional dynamic heat transfer model and a multi-dimensional coupling algorithm, enabling it to accurately handle complex heat transfer issues such as thermal bridges. Two DeST models were built for the selected building. Model 1 used the base wall K, while Model 2 used the calculated average K_m accounting for thermal bridges. Indoor environmental parameters were set according to the standard [19] and typical residential occupancy patterns. Internal heat gains from residents, lighting, and equipment were defined based on room type and schedules.

To characterize the indoor thermal environment, this experiment factored in a heat gain of 53 W/person and a moisture gain per occupant of 0.061 kg/(hr·person), while the internal gains from lighting and equipment were set at 7 W/m² and 12.7 W/m² respectively.

3.2.4. Results Analysis and Comparison

Figure 5 compares the simulated 48-hour temperature profiles for typecial room from both models with measured data. The measured temperature ranged from 5.2 °C to 7.9 °C. The overall trend of the simulated curves matched the measurements.

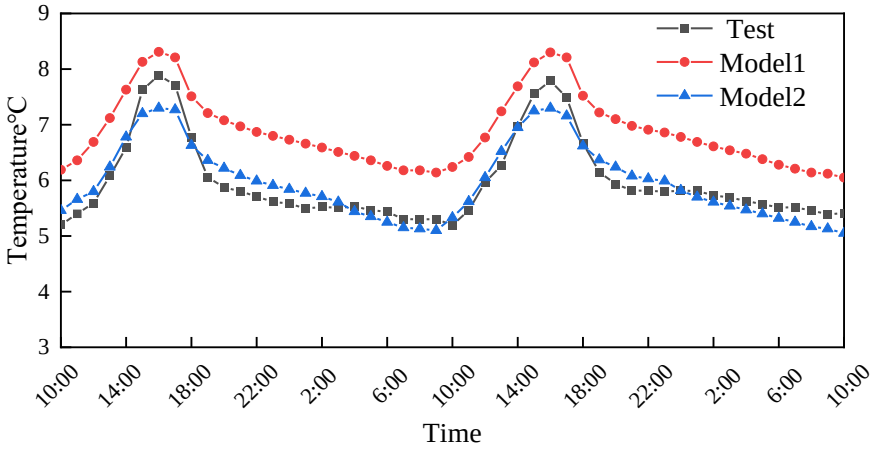

Figure 5. Temperature curves of Room.

Model 1's temperature curve was evidently higher than the measured data, with an average deviation of 0.9 °C and a mean error of 15.6%, indicating that ignoring thermal bridge effects leads to substantial inaccuracy. Model 2's average temperature was 0.9 °C (≈13%) lower than Model 1's and aligned much better with the measurements, validating the proposed calculation method. This comparison further confirms that thermal bridges significantly worsen the indoor thermal environment and increase energy consumption, highlighting that mitigating their impact can improve comfort and reduce energy use.

4. Analysis of Indoor Thermal Environment in Prefabricated Buildings

4.1. Building Model and Parameter Configuration

 doi:10.20944/preprints202603.1682.v1

Ganzi belongs to China's severe cold region C, characterized by a Qinghai-Tibet Plateau climate. This climate features low average temperatures and relatively long winters, with annual average temperatures ranging from 0.6 °C to 16.3 °C. As shown in Figure 6 (a), January is the coldest month in Ganzi with an average dry-bulb temperature of -3.7 °C, while July is the warmest month with an average dry-bulb temperature of 14.25 °C. Figure 6 (b) illustrates a frigid January with temperatures fluctuating between -10 °C and 2 °C, reaching a nadir of -9.67 °C on the 13th before rebounding. Conversely, Figure 6 (c) depicts a mild July with daily averages ranging from 9 °C to 18 °C, following an upward trend after bottoming out at 9.17 °C on the 11th. Collectively, the pronounced seasonal thermal gradient highlights the significant impact of the local climate on building thermal environments and energy demands.

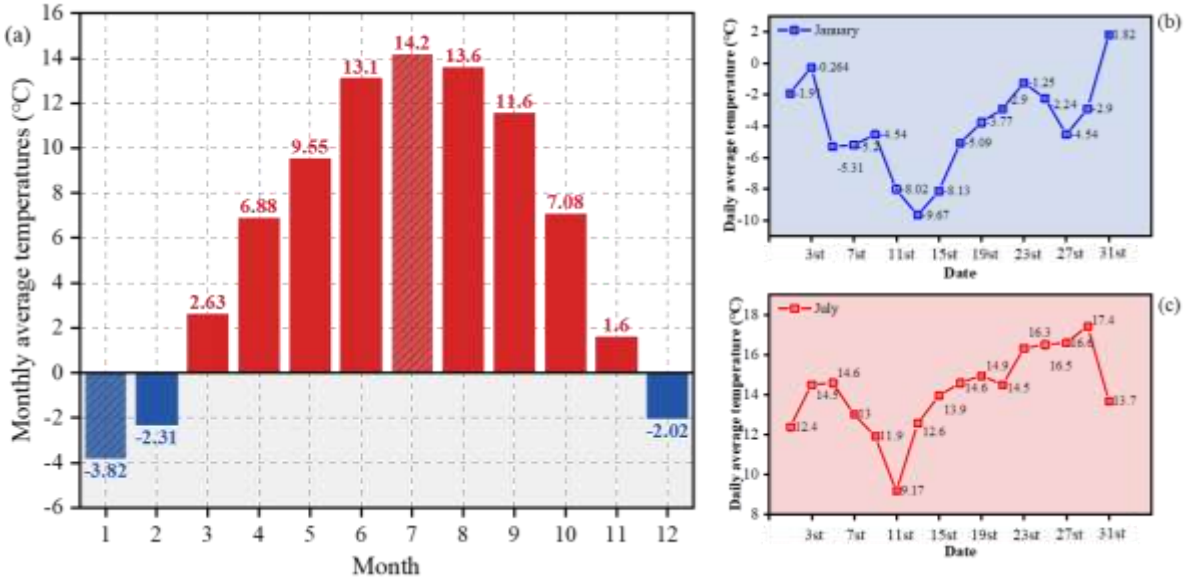

Figure 6. Ganzi Meteorological Data.

These conditions make Ganzi a representative high-altitude cold region. A newly constructed prefabricated railway building in this area was selected as the case study. A three-dimensional numerical model was established, and based on the local outdoor meteorological data and the calculation methods described previously, its annual indoor thermal environment and building energy consumption patterns, along with key influencing factors, were analyzed. The model contains two stories, each story has a floor-to-ceiling height of 3.9 m, resulting in a building shape coefficient of 0.26. The interior follows an internal corridor layout, with rooms designated by function, including a dining area, kitchen, communal laundry room, drying room, and dormitories, providing daily living space for approximately 50 people, as detailed in Figure 7. The west side of the second floor features a 10.8 m longitudinal setback serving as a living balcony. Identical window-to-wall ratios are used for both floors: 0.1 for the east and west facades, and 0.21 (north) and 0.20 (south) for the north and south facades, respectively. The structural system employs a reinforced concrete frame with precast concrete wall panels. The specific construction details and thermal parameters of the building envelope are listed in Table 2.

 doi:10.20944/preprints202603.1682.v1

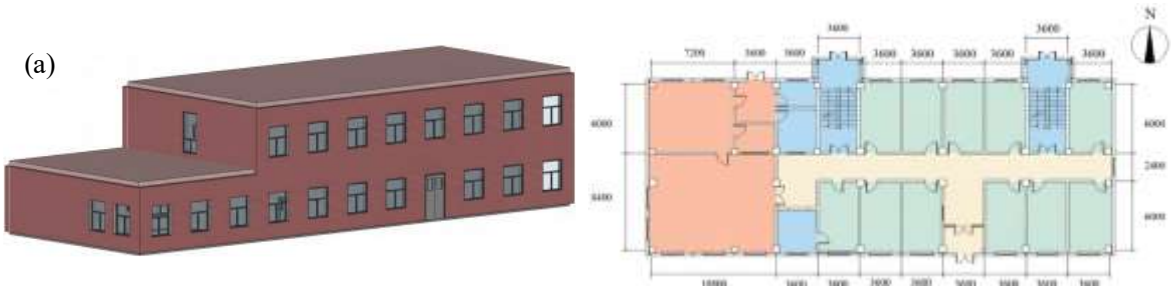

Figure 7. Rchitectural model of the railway building. (a) Architectural 3D Model (b) First Floor Plan.

Internal heat gains were defined as follows, accounting for residents, lighting, and equipment. The building serves as staff dormitories, with a maximum occupancy of two persons per room. Each resident contributes a sensible heat gain of 53 W and a moisture gain per occupant of 0.061 kg/h. The lighting power density is 7 W/m² with an electrical-to-thermal conversion efficiency of 0.9. The equipment power density is set to 12.7 W/m². To account for the impact of thermal bridges at the connection joints within the prefabricated envelope system, the linear thermal transmittance coefficients for each structural thermal bridge were calculated using PTemp, as described in the previous section. The construction details at the external wall corner and the junction between the external and internal walls are illustrated in Figure 8.

Table 2. Building Envelope Construction Details.

Category	Envelope Construction Method	Thermal Transmittance Coefficient[W/(m²·K)]
Exterior Wall	50mm recast concrete outer leaf panel + 60mm extruded polystyrene (XPS) insulation board + 120mm precast concrete inner leaf panel	0.43
Interior Wall	200mm thick aerated concrete block	1.12
Roof	40mm C20 rigid waterproof concrete topping (with ø6@100mm bidirectional reinforcement) + 3mm hemp fiber lime plaster (or paper pulp lime plaster) vapor barrier + Two layers of SBS modified bitumen waterproofing membrane (3mm each) + 25mm 1:3 cement mortar leveling screed + Minimum 30mm 1:10 cement-perlite screed at 2.5% slope + 100mm extruded polystyrene (XPS) foam insulation board + Cast-in-place reinforced concrete roof slab	0.32
Floor	120mm reinforced concrete floor slab	3.35
Exterior Window	Color 60A Series PVC-U Casement Window with Insulating Glass Unit (6mm glass + 12mm air gap + 6mm glass)	2.2~2.4

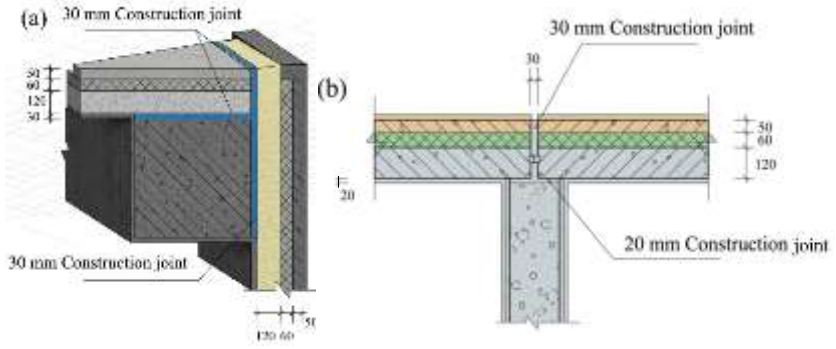

(a) **(b)**

 doi:10.20944/preprints202603.1682.v1

Figure 8. Configuration of connection between exterior walls. (a) Exterior Wall - Exterior Wall (b) Exterior Wall - Interior Wall.

4.2. Simulation Results

Rooms were categorized by orientation: north-facing rooms on the first floor, south-facing rooms on the first floor, north-facing rooms on the second floor, and south-facing rooms on the second floor. The annual indoor temperature statistics for each category are summarized in Table 3. According to the Chinese National Standard GB5009-2003 Code for Design of Heating, Ventilation and Air Conditioning, the acceptable indoor temperature range for primary rooms in civil buildings is 18–24 °C. The statistical analysis reveals that for all north-facing rooms, indoor temperatures fell outside this comfort range for 60.49% of the year, with an annual average temperature of 12.95 °C. For all south-facing rooms, temperatures were outside the comfort range for 49.76% of the year, with a higher annual average of 15.29 °C. This indicates a significant influence of orientation on the indoor thermal environment. In contrast, the impact of floor level was minimal. For instance, the difference in the percentage of discomfort level between first-floor and second-floor north-facing rooms was only about 1%, with a negligible mean temperature difference of 0.01 °C. Aggregating data from all rooms shows that indoor temperatures failed to meet the comfort threshold that is below 16 °C for 54.43% of the year, consistently skewing towards the cold side. This result confirms that the current indoor thermal conditions are insufficient for residents' daily comfort needs. Consequently, further analysis of factors such as the window-to-wall ratio and the thermal performance of the building envelope is required to explore potential improvements in comfort.

Table 3. Indoor Temperature Distribution Statistics.

Room Orientation	Temperature Range /℃	Time Percentage /%	Average Temperature /℃
North-facing rooms on the 1st floor	<16	61.54	12.94
	16~28	38.46	
South-facing rooms on the 1st floor	<16	51.36	15.23
	16~28	48.64	
North-facing rooms on the 2nd floor	<16	59.45	12.95
	16~28	40.55	
South-facing rooms on the 2nd floor	<16	48.77	15.32
	16~28	51.23	
North-facing total	<16	60.49	12.95
	16~28	39.51	
South-facing total	<16	49.76	15.29
	16~28	50.24	
Total	<16	54.43	14.27
	16~28	45.57	

Figure 9 illustrates the annual load simulation results for the baseline model. The cooling season was defined from June 1st to August 31st, while the heating season spanned from November 15th to March 15th of the following year. As shown, the building exhibits zero cooling demand throughout the year, with thermal loads heavily concentrated within the heating season, validating the accuracy of the numerical simulation. Simulation data indicate that the peak heating load of 76.55 kW occurred in January. Calculations show the initial model's annual cumulative load totaled 50,504.11 kWh.

 doi:10.20944/preprints202603.1682.v1

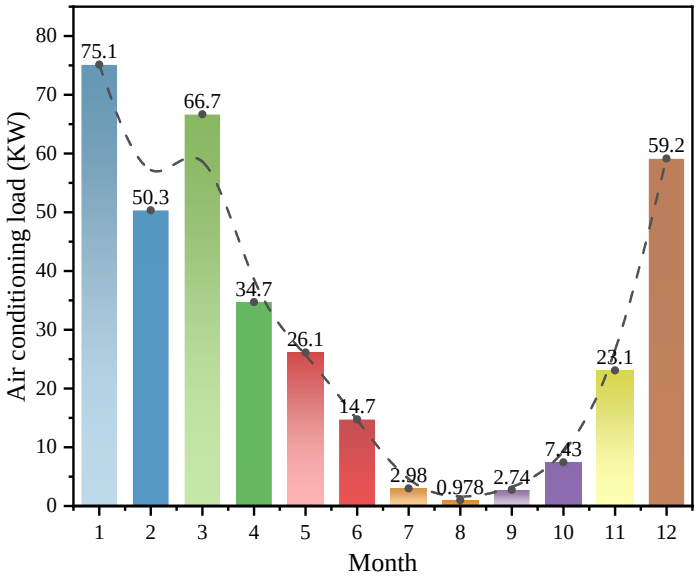

Figure 9. Hourly Air Conditioning Load Throughout the Year.

4.3. Analysis of Key Influencing Factors

4.3.1. Building Orientation

Building orientation is a key factor influencing the indoor thermal environment [21], primarily affecting indoor temperature through its impact on solar radiation heat gain, which in turn determines building energy consumption. In winter, solar heat gain can effectively reduce the space heating load. Therefore, considering the variation patterns of solar azimuth and altitude angles, buildings oriented along the north-south axis receive greater solar radiation. To determine the most suitable building orientation for the Ganzi region, a comprehensive simulation was conducted. The full 360° range was divided into 24 groups at 15° intervals to investigate the influence of orientation on indoor comfort and energy consumption. The south-facing wall was defined as the reference plane (i.e., building facade), corresponding to 0° orientation. The orientation angle increases clockwise: 90° for west-facing, 180° for north-facing, and 270° for east-facing. Simulation results for all rooms under each of the 24 orientation groups are presented in Figure 10.

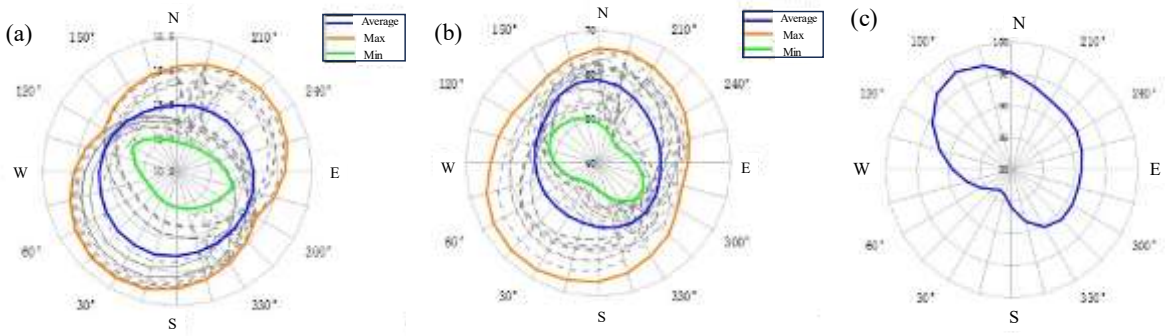

Figure 10. Effect of the building orientation. (a) Average temperature (b) Discomfort Level (c) Building Energy Consumption.

From a holistic building perspective, the impact of orientation on the average indoor temperature and discomfort level was analyzed. In Figure 10(a), the dashed lines illustrate the variation in the annual average indoor temperature for each of the 23 dormitory rooms. As the orientation changes, indoor temperatures on the south-facing side show a significant increase. The

 doi:10.20944/preprints202603.1682.v1

maximum and minimum temperature curves reveal that the greatest difference in annual average temperature among the dormitories occurs at a 45° orientation, reaching 4.1 °C, while the smallest difference of 1.4 °C occurs at 120°. Furthermore, considering the average temperature across all 23 rooms, the highest and lowest values are 14.3 °C and 13.4 °C, corresponding to orientations of 15° and 180°, respectively. Figure 10(b) shows the annual percentage of discomfort level for each room. The average discomfort level is highest (58.83%) when the building faces 180° (north), and lowest (53.6%) at a 30° orientation. Figure 10(c) presents the overall building energy consumption curve. Energy consumption peaks at a 150° orientation, with an annual cumulative load of 57,351.41 kW·h and a unit area load of 97.62 kW·h/m². Conversely, the minimum energy consumption occurs at 30°, with an annual cumulative load of 49,129.26 kW·h and a unit area load of 83.62 kW·h/m², representing a significant reduction of 14.4%. This clearly demonstrates the substantial influence of building orientation on energy consumption. Considering factors such as average indoor temperature, comfort level, and energy consumption, the optimal orientation range for this building in the Ganzi region is between 15° and 45°, while the least favorable range is between 135° and 180°.

4.3.2. South-Facing Window-to-Wall Ratio

Research indicates that for severely cold and cold regions, appropriately increasing the south-facing window-to-wall ratio (WWR) can enhance indoor comfort and reduce energy consumption [22]. The building's layout is elongated along the east-west axis with a shorter north-south depth, and the number of windows on the east and west façades is considerably lower than those on the north and south. Given the greater influence of the south-facing WWR, the simulation analysis focused exclusively on this parameter. The south-facing WWR was varied from 0.10 to 0.45 to investigate its impact on annual indoor discomfort levels and building energy consumption.

Based on the analysis results in Figure 11(a), a linear relationship can be observed between the increase in the south-facing window-to-wall ratio and building energy consumption, manifested as a gradual reduction in energy use. When the window-to-wall ratio reaches 0.45, the building energy consumption reaches its minimum, with a unit area load of 68.69 kW·h/m². In contrast, at a window-to-wall ratio of 0.1, the energy consumption is at its maximum, with a unit area load of 99.21 kW·h/m², representing an increase of 44.43% compared to the minimum. This result further confirms the significant impact of the south-facing window-to-wall ratio on building energy consumption. Concurrently, indoor discomfort continuously decreases as the south-facing window-to-wall ratio increases, reaching a minimum of 45.37% at a ratio of 0.45, while the annual average temperature across all rooms is 15.71 °C. At a window-to-wall ratio of 0.1, indoor discomfort peaks at 60.41%, with an annual average temperature of 13.28 °C. The difference in discomfort levels is approximately 15%, while the difference in average temperature is as high as 2.43 °C.

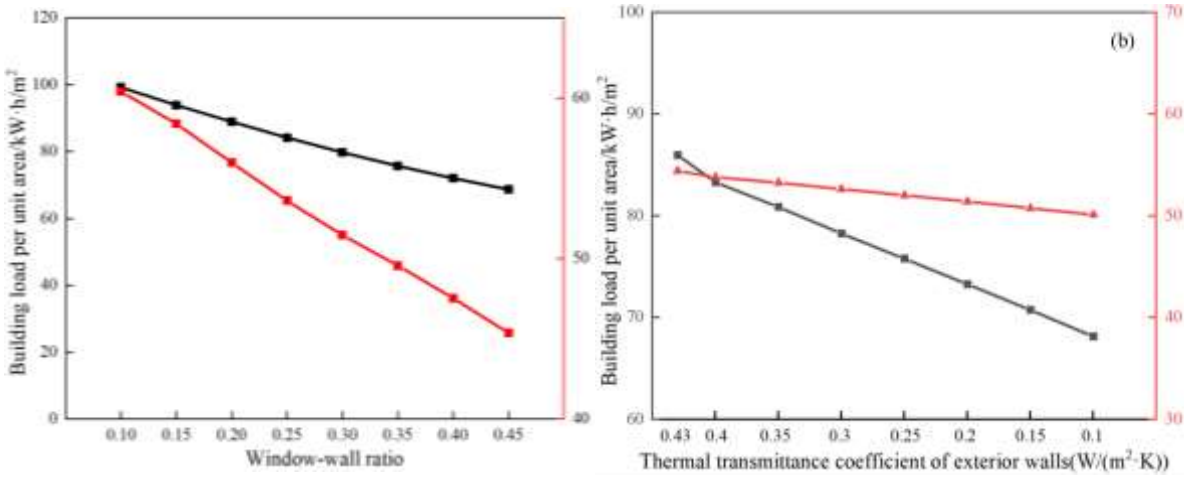

Figure 11. South-Facing Window-to-Wall Ratio results. (a) Effect of south-facing window-to-wall ratio (b) Effect of heat transfer coefficient of the exterior wall.

 doi:10.20944/preprints202603.1682.v1

Considering the trends in both energy consumption and comfort, it is evident that the south-facing window-to-wall ratio exerts a substantial influence on the overall building performance. This factor must be comprehensively evaluated during design and reasonably determined within regulatory limits. According to solar resource analysis for the Ganzi, the region receives total solar radiation generally between 5000 and 6800 W/m², with annual sunshine hours ranging from 2000 to 2600 hours and a sunshine percentage exceeding 40%, indicating exceptionally abundant solar resources. Therefore, in high-altitude cold regions such as Ganzi, despite low ambient temperatures, appropriately increasing the south-facing window-to-wall ratio can maximize the utilization of these abundant solar radiation resources. However, as windows represent a thermal weak point in the envelope, an excessively high window-to-wall ratio may introduce excessive solar radiation during the day, leading to indoor overheating, while allowing greater heat loss at night, resulting in a colder perceived temperature and discomfort. Furthermore, glare may occur around midday, particularly in summer, impairing the indoor visual environment and affecting the living experience. Consequently, for prefabricated railway buildings in the Ganzi region, and in accordance with regulatory requirements, the south-facing window-to-wall ratio should preferably be set between 0.35 and 0.45.

 doi:10.20944/preprints202603.1682.v1

4.3.3. Exterior Wall Thermal Transmittance

As exterior walls constitute the largest portion of the building envelope's surface area, heat loss through them accounts for a significant proportion of the total building heat loss. Their thermal performance directly affects the indoor thermal environment and the energy required for heating and cooling. This is especially critical in severe cold and cold regions, where enhancing the thermal insulation performance of the building envelope is key to improving indoor comfort and reducing energy consumption [23,24]. By adjusting the thickness of the insulation layer in a sandwich wall assembly, the exterior wall's thermal transmittance coefficient K can be modified. Based on the method previously described, the average thermal transmittance coefficient K_m of the exterior wall was calculated to investigate the impact of the wall's thermal performance on the indoor environment and building energy consumption. In the baseline model, the exterior wall consists of a 60 mm thick extruded polystyrene (XPS) insulated sandwich panel, with a thermal transmittance coefficient K = 0.43 W/(m²·K). Considering thermal bridge effects, the calculated average thermal transmittance is K_m = 0.463 W/(m²·K). Assuming the wall's K is reduced from 0.43 to 0.1, the average K_m continuously decreases, while the indoor average temperature correspondingly increases. Both the discomfort level and the building load per unit area show a linear decreasing trend, as illustrated in Figure 11(b). Specifically, the unit area load decreases significantly from 85.96 kW·h/m² to 68.13 kW·h/m², a reduction of 20.7%. The average indoor temperature increases by 0.77 °C, and the discomfort percentage drops from 54.43% to 50.11%, a decrease of 7.9%. This indicates that reducing the average thermal transmittance of the exterior wall has a greater effect on lowering building energy consumption than on raising the average indoor temperature.

Building upon this foundation, and to further optimize the wall construction for practical guidance, the wall thickness was adjusted using DeST software. While keeping the materials of the inner and outer wythes unchanged, the thickness of the extruded polystyrene insulation layer was varied. The resulting relationship between insulation thickness and the wall's thermal transmittance coefficient is shown in Figure 12. As shown in the figure, increasing the insulation thickness δ reduces the wall's K. When δ is less than 60 mm, the K decreases sharply with increasing δ. However, once δ exceeds 60 mm, the rate of decrease in the K gradually slows with further increases in thickness. When δ is greater than 120 mm, the K drops to approximately 0.2 W/(m²·K), and its change approaches an asymptotic limit, becoming almost unaffected by additional insulation. Although Figure 9 indicates that achieving a K of 0.2 significantly improves indoor comfort and reduces energy consumption, a comprehensive consideration of economic cost and building space efficiency suggests that an insulation thickness between 60 mm and 120 mm is advisable for exterior walls in high-altitude cold regions.

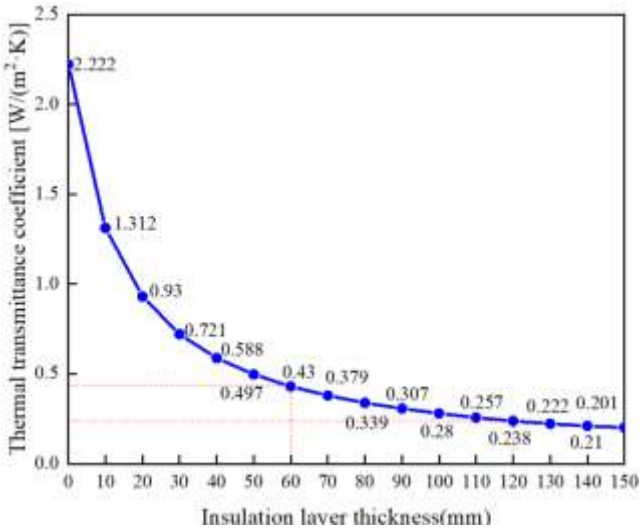

 doi:10.20944/preprints202603.1682.v1

Figure 12. Variation of heat transfer coefficient of the exterior wall.

4.4. Impact of Exterior Window Thermal Transmittance on Indoor Thermal Environment and Energy Consumption

As the weakest joint in the building envelope, the thermal performance of exterior windows significantly impacts both building energy consumption and indoor thermal comfort. This section simulates eight sets of data for window *K* ranging from 2.3 W/(m²·K) to 1.0 W/(m²·K), analyzing their effects on average indoor temperature, indoor discomfort levels, and annual building energy consumption. The distribution of discomfort temperature percentages and building loads under varying window-to-wall ratios was compiled. A line chart was used to visually illustrate the impact of window-to-wall ratio on room comfort and building energy consumption, with results shown in Figure 13(a).

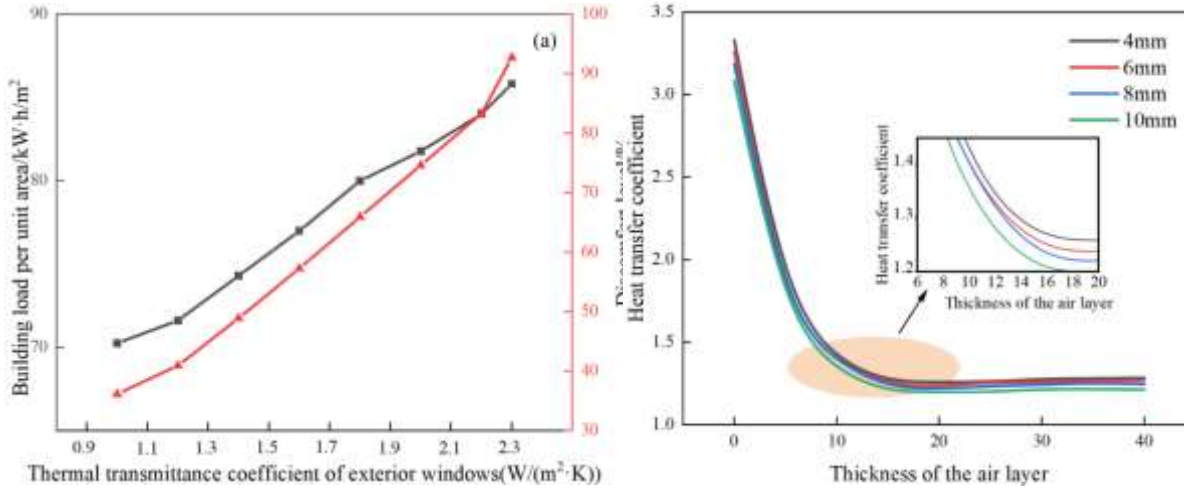

Figure 13. Impact of Exterior Window Thermal Transmittance. (a) Indoor discomfort and building energy consumption under different heat transfer coefficients of exterior walls (b) The variation law of heat transfer coefficient of exterior windows.

It can be observed that as the thermal transmittance coefficient of exterior windows decreases, building energy consumption exhibits a linear downward trend, reaching its minimum value when the thermal transmittance coefficient is 1.0 W/(m²·K), at which point the building load per unit area is 70.40 kW·h/m². When the thermal transmittance coefficient of exterior windows is 2.3 W/(m²·K), corresponding to the initial model, building energy consumption reaches its maximum value, with a building load per unit area of 85.96 kW·h/m², representing a 22.10% increase. This demonstrates that reducing the thermal transmittance coefficient and improving the thermal insulation performance of exterior windows significantly impacts the reduction of building energy consumption. Similarly, indoor discomfort levels exhibit a linear decrease as the exterior wall *K* decreases, reaching a minimum at a *K* of 1.0 W/(m²·K), where indoor discomfort is 50.53%. The annual average temperature across all rooms was 14.97 °C. When the thermal transmittance coefficient of exterior windows reached 2.3 W/(m²·K), indoor discomfort peaked at 54.43%. The annual average temperature across all rooms was 14.27 °C. The difference in discomfort levels was approximately 4%, while the average temperature difference was 0.70 °C.

Considering both energy consumption and comfort levels, the thermal transmittance coefficient of exterior windows significantly impacts the overall building performance. Standard single-pane exterior windows typically have a thermal transmittance coefficient ranging from 2.0 W/(m²·K) to 4.2 W/(m²·K). while standard double-glazed windows typically range from 1.8 W/(m²·K) to 3.4 W/(m²·K). For energy-efficient windows, the *K* generally falls between 1.4 W/(m²·K) and 1.8 W/(m²·K). As shown in Figure 13 (b), when the thermal transmittance approaches 1.4 W/(m²·K), further reducing the thermal transmittance of exterior windows by increasing air thickness becomes impractical.

 doi:10.20944/preprints202603.1682.v1

Therefore, considering cost-effectiveness, a thermal transmittance range of 1.4 W/(m²·K) to 1.6 W/(m²·K) is deemed appropriate for prefabricated railway residential buildings in the Ganzi region.

5. Specific Measures for Railway Building Envelopes in the Western Sichuan Plateau Region

5.1. Thermal Performance Design for Typical Regions

5.1.1. Analysis Scheme

To further define the thermal environment design parameters for buildings along the plateau railway, this study selected a railway line in the Western Sichuan region of China as the research subject. The chosen railway traverses the Western Sichuan Plateau and the Tibetan Plateau, specifically covering the stations of Litang and Batang located on the Western Sichuan Plateau, as well as Qamdo, Nyingchi, and Lhasa located on the Tibetan Plateau, as shown in Figure 14. Based on the optimal energy consumption and indoor discomfort parameters for the Garzê region, as discussed in Section 4, simulation designs were conducted using an orthogonal array L9 (3^4) that accounts for multiple factors at consistent levels. The analysis focused on the indoor thermal environment design parameters for different areas along the railway, with detailed results presented in Tables 4 and 5.

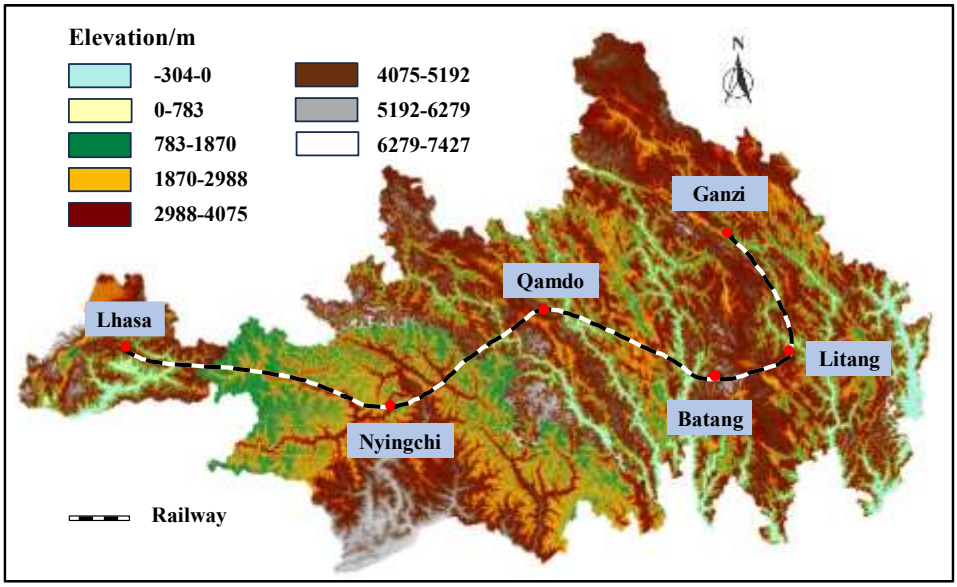

Figure 14. Location, topography, and geological map of the study area.

Table 4. Simulation Scheme.

Model \ Factor	Orientation /°	South-facing Window-to-Wall Ratio	Average Thermal Transmittance of Exterior Walls [W/(m²·K)]	Thermal Transmittance Coefficient of Exterior Windows [W/(m²·K)]
Model 1	Condition 1	Condition 4	Condition 7	Condition 10
Model 2	Condition 1	Condition 5	Condition 8	Condition 11
Model 3	Condition 1	Condition 6	Condition 9	Condition 12
Model 4	Condition 2	Condition 4	Condition 9	Condition 12
Model 5	Condition 2	Condition 5	Condition 8	Condition 10
Model 6	Condition 2	Condition 6	Condition 7	Condition 11
Model 7	Condition 3	Condition 4	Condition 9	Condition 11
Model 8	Condition 3	Condition 5	Condition 7	Condition 12

 doi:10.20944/preprints202603.1682.v1

Model 9	Condition 3	Condition 6	Condition 8	Condition 10

Table 5. Operating Condition Table.

Region	Cond. 1	Cond. 2	Cond. 3	Cond. 4	Cond. 5	Cond. 6	Cond. 7	Cond. 8	Cond. 9	Cond. 10	Cond. 11	Cond. 12
Litang	SW15°	SW30°	SW45°	0.35	0.40	0.45	0.05	0.10	0.15	1.0	1.1	1.2
Batang	S	SW15°	SW30°	0.35	0.40	0.45	0.40	0.45	0.50	2.0	2.2	2.4
Qamdo	S	SW15°	SW30°	0.35	0.40	0.45	0.25	0.3	0.35	1.4	1.6	1.8
Nyingch	S	SW15°	SW30°	0.35	0.40	0.45	0.45	0	0.50	2.0	2.2	2.4
Lhasa	S	SW15°	SW30°	0.35	0.40	0.45	0.25	0.30	0.35	1.4	1.6	1.8

5.1.2. Regional Thermal Performance Analysis

For the Litang region, Figure 15 shows that Model 3 yields the best results when considering indoor discomfort, with a discomfort level of only 33.92%. However, its annual cumulative load per unit area is 43.22 kW·h/m², which exceeds the annual limit of 40 kW·h/m². When considering only building energy consumption, Model 6 performs best, with an annual load of 37.11 kW·h/m² (below the 40 kW·h/m² limit) and an indoor discomfort level of 36.67%, though its average exterior wall thermal transmittance is relatively low. A comprehensive comparison reveals that Model 9 not only meets the energy limit but also achieves higher indoor average temperatures and comfort levels. Moreover, its average wall thermal transmittance is higher than that of Model 6, making it more cost-effective. In Batang, Model 6 achieves an annual load of 38.72 kW·h/m², falling short of the 40 kW·h/m² limit by 3.20%, with an indoor discomfort level of 30.01%. When both discomfort and average temperature are considered, Model 9 is again optimal, showing a discomfort level of 29.78%, an annual average indoor temperature of 19.11 °C, and an annual load of 40.55 kW·h/m²-only 1.37% above the limit. Similar analyses were conducted for the Qamdo, Nyingchi, and Lhasa regions.

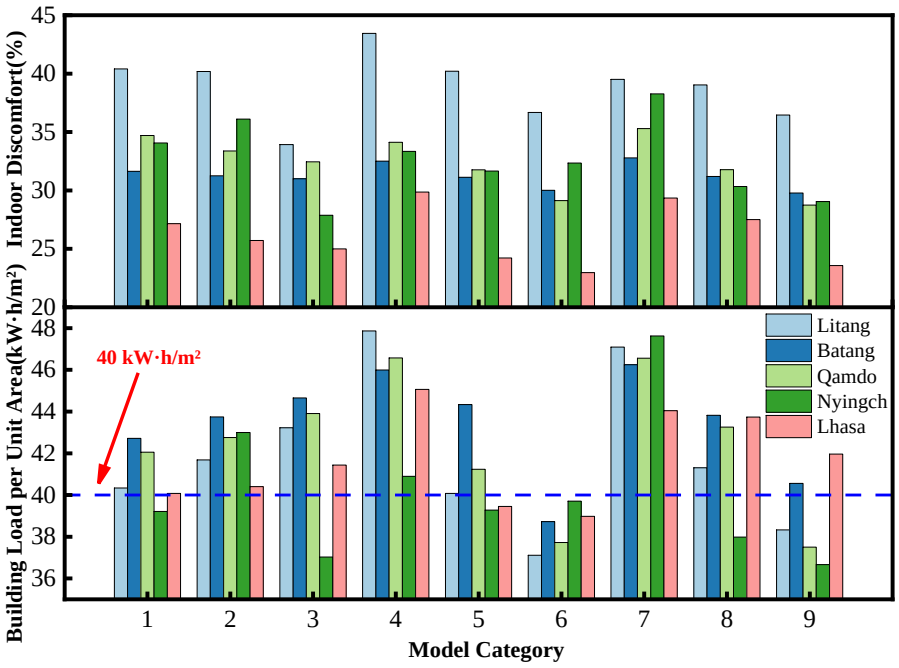

Figure 15. Thermal Analysis Results for a Typical Region.

 doi:10.20944/preprints202603.1682.v1

5.2. Analysis Results

5.2.1. Building Orientation

Appropriate building orientation significantly improves the indoor thermal environment, enhances residents' thermal comfort, reduces building energy consumption, and consequently lowers overall energy use. The optimal orientations for each station are summarized in Table 6.

Table 6. Optimal Building Orientations for Sites Along the Route.

Region	Optimal Orientation (°)
Litang	SW 45
Batang	SW 30
Qamdo	SW 15
Nyingchi	SW 30
Lhasa	SW 30

According to the results presented, the optimal building orientation for the Western Sichuan Plateau region falls within the range of 30° to 45° west of south. For the Tibetan Plateau region, the optimal range is between 15° and 30° west of south. Along the railway route, where latitude remains largely constant while longitude decreases, the variation in optimal orientation remains within 30°. The simulation results indicate that orientation changes within a 15° range have a relatively minor impact on building energy consumption and indoor comfort, with an effect of less than 5%. However, a larger change, such as shifting the orientation from south to north, can increase energy consumption by approximately 20%. Since adjusting building orientation typically incurs no additional cost or effort, orientation analysis should be conducted during the architectural design phase in practical projects to determine the optimal alignment. Furthermore, in high-altitude cold regions, a primary south-facing orientation can better utilize solar resources, for instance, by implementing direct-gain solar rooms or using thermal mass walls on the south façade, to enhance indoor thermal comfort and reduce energy consumption. For this prefabricated railway building, the internal corridor layout results in significantly higher average temperatures and comfort levels in south-facing rooms compared to north-facing ones. Therefore, during design, rooms with lower occupancy rates, such as storage rooms, preparation areas, and laundry rooms, can be positioned on the north side to maximize the thermal environment in primary living spaces. In summary, for prefabricated railway living quarters along this route, the overall optimal building orientation shows limited variation, generally distributed between 15° and 45° west of south.

5.2.2. Average Thermal Transmittance Coefficient of Exterior Walls

As shown in Table 7, the optimal thermal transmittance coefficient K for exterior walls along the railway route does not follow a clear geographical pattern. From the Ganzi region to Litang, the optimal K decreases gradually from 0.15 W/(m²·K) to a minimum of 0.10 W/(m²·K). From Litang to Batang, it then increases, reaching a maximum of 0.65 W/(m²·K) in Batang. Entering the Tibetan Plateau from the Western Sichuan Plateau, the value decreases again, dropping to 0.30 W/(m²·K) in Qamdo. From Qamdo to Nyingchi, it increases to 0.50 W/(m²·K), and finally, the optimal K in Lhasa is 0.45 W/(m²·K).

Table 7. Thermal Transmittance Coefficients of Exterior Walls at Sites Along the Route.

Region	Optimal Exterior Wall Thermal Transmittance Coefficient [W/(m²·K)]	Optimal Average Exterior Wall Thermal Transmittance Coefficient [W/(m²·K)]
Litang	0.10	0.107
Batang	0.65	0.702

 doi:10.20944/preprints202603.1682.v1

Qamdo	0.30	0.320
Nyingchi	0.50	0.539
Lhasa	0.45	0.483

The variation in optimal *K* is primarily attributable to differences in solar radiation intensity and outdoor temperature. For instance, Litang not only has the highest elevation but also receives the weakest solar radiation, resulting in the most severe outdoor environment. A lower *K* provides effective thermal insulation under these conditions. In contrast, Batang has the lowest elevation but an annual average direct solar radiation intensity of 118.35 W/m², approximately 70% higher than that in Litang. Therefore, considering cost-effectiveness, a relatively higher wall thermal transmittance can be adopted. Furthermore, for the Batang region, a higher *K* can also help maintain indoor thermal comfort and reduce cooling energy consumption during summer.

5.2.3. Thermal Transmittance of Exterior Windows

As transparent components of the building envelope, exterior windows typically have higher thermal transmittance coefficients than walls, making them a potential thermal weak point. However, they also allow greater solar heat gain during daytime, which can raise indoor temperatures and improve the thermal environment. Additionally, windows provide essential daylighting and ventilation. Appropriate window selection significantly enhances residents' comfort and well-being. The optimal thermal transmittance coefficients for exterior walls at each station along the route are summarized in Table 8.

Table 8. Optimal Exterior Window Thermal Transmittance Coefficients for Sites Along the Route[W/(m²·K)].

Region	Optimal Exterior Window Thermal Transmittance Coefficient
Litang	1.0
Batang	3.0
Qamdo	1.8
Nyingchi	2.4
Lhasa	2.2

As indicated in the corresponding results, the variation pattern of the optimal thermal transmittance coefficient for exterior windows along the railway route is generally similar to that of the exterior walls. Specifically, from the Ganzi region to Litang, the *K* decreases gradually from 1.4 W/(m²·K) to a minimum of 1.0 W/(m²·K). It then rises to a maximum of 3.0 W/(m²·K) in Batang. Upon entering the Tibetan Plateau region, the K gradually decreases, dropping to 1.8 W/(m²·K) in Qamdo. From Qamdo to Nyingchi, it increases again to 2.4 W/(m²·K), and finally, the optimal *K* in Lhasa is 2.2 W/(m²·K). The variation in the optimal window thermal transmittance is primarily driven by changes in solar radiation intensity and outdoor temperature. When solar radiation is weak and the average outdoor temperature is low, a lower window *K* helps minimize indoor heat loss. Conversely, under conditions of strong solar radiation and higher average temperatures, a higher window *K* is more advantageous, both from an economic standpoint and in terms of beneficial solar heat gain.

6. Conclusions and Recommendations

This study focuses on the indoor thermal environment of prefabricated railway living quarters in high-altitude cold regions. Through theoretical simulation and parameter optimization, it systematically reveals the influence patterns of thermal bridge effects, building orientation, south-facing window-to-wall ratio, and exterior wall thermal transmittance on thermal comfort and energy consumption, providing a quantitative basis and optimization pathways for the thermal design of railway station buildings in such areas.

 doi:10.20944/preprints202603.1682.v1

(1) The calculation method utilizing the average thermal transmittance coefficient, which accounts for structural thermal bridges, enables effective simulation of thermal bridge effects in the building envelope. Comparison with field measurement data confirms that this method can accurately reflect the actual impact of these effects on the indoor thermal environment and building energy consumption.

(2) The annual average indoor temperatures in the primary rooms were generally low. South-facing rooms exhibited an average temperature 2.3℃ higher than north-facing rooms, and the annual percentage of time failing to meet comfort requirements was 17.74% less for south-facing rooms. Consequently, the local average temperature distribution within the building varies significantly depending on room orientation.

(3) Building orientation, south-facing window-to-wall ratio, and exterior wall thermal performance significantly influence the building's global average temperature and energy consumption. For the computational model in this study, the optimal orientation range is 15°–45°, while the least favorable range is 135°–165°. It is recommended to set the south-facing window-to-wall ratio between 0.35 and 0.45. Optimizing the thermal transmittance coefficient can be achieved by increasing the insulation layer thickness. For exterior walls constructed with precast concrete inner and outer wythes and an extruded polystyrene insulation core, an insulation thickness of 60–120 mm is advised.

(4) For the Western Sichuan Plateau region; the optimal building orientation ranges from 30° to 45° west of south. For the Tibetan Plateau region; the optimal range is from 15° to 30° west of south. The optimal thermal transmittance coefficients for exterior walls in the studied regions are 0.15; 0.10; 0.65; 0.30; 0.50; and 0.45 W/(m²·K); respectively; indicating the substantial influence of altitude and solar radiation intensity on the wall envelope performance. Correspondingly; the optimal thermal transmittance coefficients for exterior windows are 1.4; 1.0; 3.0; 1.8; 2.4; and 2.2 W/(m²·K)

This study investigated the energy consumption characteristics of prefabricated exterior walls in high-altitude railway buildings by simulating their thermal performance, with particular emphasis on the average heat-transfer coefficient to analyze thermal-bridge effects. Measures to improve the indoor thermal environment of buildings in plateau regions were proposed. This study still has several limitations that need to be addressed and improved in future research. Future research should prioritize long-term field measurements in typical plateau areas to validate the quantitative thermal-bridge models and dynamic response patterns of prefabricated envelopes identified in this study. The research scope should further incorporate a human-centered perspective, integrating physiological and psychological feedback from occupants to develop a comfort evaluation system tailored to low-pressure, low-oxygen plateau environments, thereby promoting the sustainable green development of railway station buildings in high-altitude regions.

CRediT authorship contribution statement: Hui Li: Writing – review & editing, Methodology, Supervision, Conceptualization, Validation. **Lintao Ma:** Writing – review & editing, Supervision, Validation. **Haojie Zhang:** Writing – original draft, Data curation, investigation. **Zhixiang Yu:** Supervision, Validation, Funding administration. **Hu Xu:** Writing – original draft, Data curation.

Declaration of Competing Interest: The authors declare that they have no known competing financial interests or personal relationships that could have appeared to influence the work reported in this paper.

Data Availability: Data will be made available on request.

Acknowledgments: The authors are grateful for the support of the Foundation for Technology Development Project of China Railway First Survey and Design Institute Group Co., Ltd. (No. 19-44).

 doi:10.20944/preprints202603.1682.v1

References

1. LI Fangde, ZHANG Weijie, WANG Yan, et al. Building energy-saving retrofit and application analysis of prefabricated building in rural areas in hot summer and warm winter areas [J]. Building Structure, 2021, 51(S1): 1059-1065.
2. Yan Han. Discussion on the Application of Prefabricated Construction Mode inPlateau Railway Building [J]. Construction Science and Technology, 2021,444(12): 7-11.
3. Li Jinping, Wang Zhaofu, Wang Hang, et al. Research on indoor comfort of active and solar cooperative heating in cold Tibetan region[J]. Journal of Xi'an University of Architecture and Technology (Natural Science Edition), 2019, 51(4): 584-590.
4. Ganlin Zhang. Regional Adaptability of Tibetan Dwelling in East Khams, Ganzi*[D]. Shaanxi: Xi'an University of Architecture and Technology, 2019.
5. Jiawen Hou. Optimization of indoor thermal environment in winter for traditional Tibetan dwellings in the Sichuan northwestern plateau[D]. Sichuan Agricultural University, 2019.
6. WANG Chaohong, YANG Yang, WEI Guanglong. Study on the optimization of additional sunspace of rural residences in cold regions based on benefit evaluation[J]. Building Science,2023,39(04):130-138.
7. LIAN Zhiwei, CAO Bin, DU Heng, et al. Determination method of comfortable zone for indoor thermal environment[J]. Building Science,2022,38(08):9-14+22.
8. Zhu Xiaolin. Research and Evaluation on Thermal Insulation Performance of the external Envelope Structure of the Fabricated Composite Wall Structure System Dwellings [D]. Shaanxi: Xi'an University of Architecture and Technology, 2018.
9. Ju Bin. Research on energy saving technology of prefabricated building envelope structure in cold region [D]. Shaanxi: Xi'an University of Science and Technology, 2018.
10. Yang Jingbo. Analysis and Improvement of Thermal Bridge of Building Envelope Based on a Prefabricated Building [D]. Hunan: Hunan University, 2019.
11. HU Tianhe, HU Redundancy, HU Wei. Research on thermal bridge of dry connection with vertical joint for prefabricated wall structure[J]. Industrial Building, 2020, 50(07): 72-76.
12. Scioti A., De Fino M., Martiradonna S., et al. Construction Solutions and Materials to Optimize the Energy Performances of EPS-RC Precast Bearing Walls[J]. Sustainability, 2022, 14(6): 3558.
13. N.Bouchlaghem. Optimising the design of building envelopes for thermal performance[J]. Automation in Construction, 2020(10):101-112.
14. Yu SS, Liu YF, Wang, DJ, et al. Review of thermal and environmental performance of prefabricated buildings: Implications to emission reductions in China[J]. Renewable & Sustainable Energy Reviews, 2021, 137:110472.
15. YINQUAN YU, XIAO MING, WANG Zhan, et al. Research on seam width of precast concrete facade panel [J]. Building Structure,2019,49(11): 1-8.
16. Liu Xuan. Energy Consumption Test and Energy Saving Optimization of Assembled Low Energy Consumption Residential Buildings in Cold Regions [D]. Shandong: Yantai University, 2020.
17. Sun Daming, Zhou Hai Zhu, Tian Huifeng. Tian Huifeng. Research status and prospect of building thermal bridge [J]. Building Science, 2010, 26(02): 128-134.
18. GU Hao-Sheng, LU Duan-Wei, WANG Qi. Design of ultra-low energy precast concrete residences [J]. Building Structure, 2021, 51(S1): 1066-1070.
19. Thermal design code for civil building: GB50176-2016 [S]. Beijing: China Construction Industry Press, 2016.
20. ZHU Xiaolin, HU Redundancy, LIU Jiaping. Research on Indoor Thermal Environment Test of Prefabricated Civil Residence in Winter[J]. Residential Science and Technology,2018,38(09): 28-32.
21. Zhang Yiping, Li Yourong, Wang Jinxin, et al. Preliminary analysis of indoor temperature and humidity characteristics of a low-latitude plateau city with north-south orientation in winter[J]. Journal of Tropical Meteorology,2001,17(03): 36-40.
22. Li Zhengrong, Siyang, Zhao Qun, et al. Suggestions on Retrofitting the wall thermal inertia index for non-heated traditional house in tibet[J]. Building Energy Conservation,2020,48(12): 36-40.

 doi:10.20944/preprints202603.1682.v1

23. Sarkar A., Bose S.. Exploring impact of opaque building envelope components on thermal and energy performance of houses in lower western Himalayans for optimal selection[J]. Journal of Building Engineering. 2016, 7:170-182.
24. Chen Jie, Yang Liu, Luo Zhixing. Analysis of indoor thermal environment of residential buildings in Turpan[J]. Journal of Xi'an of Arch and Tech (Natural Science Edition), 2019, 51(4): 578-583.